Siloxanes capture by Ionic Liquids: Solvent Selection and Process Evaluation

Rubén Santiago*, Cristian Moya, and José Palomar

Chemical Engineering Department. Universidad Autónoma de Madrid. 28049 Madrid. Spain

*E-mail corresponding author: ruben.santiago@uam.es

Keywords: Siloxanes; Ionic Liquids; Absorption; Biogas

Abstract

Nowadays, new technologies are being developed to substitute conventional energy resources. Biogas has emerged to avoid the intensification of global warming and promote waste valorization. However, undesirable chemicals must be removed prior to its utilization. Siloxanes stand out as biogas contaminants since they can damage process equipment's. Therefore, in this work, COSMO-based/Aspen Plus computational methodology was applied to evaluate as first-time, ionic liquids (ILs) as siloxanes absorbents on biogas upgrading context. Thus, molecular simulation using COSMO-RS method was used to analyze the interactions between siloxanes/ILs based on excess properties. Moreover, it was used to select the most promising ILs among a wide sample (900) of solvents for latter process simulation stage based on thermodynamics (Henry's law constants) and kinetics (low viscosity). The results revealed that ILs with fluorinated anions are the best for the task. Then, the performance of selected ILs on siloxane capture at industrial scale was evaluated by means of Aspen Plus process simulations. Thus, the absorption efficiency in a packed column was analyzed by comparing the silicon concentration in outlet gas stream for each IL, using a rigorous RADFRAC column in Rate-base mode. Operating pressure inside the column was also studied as key operating variable. Last, simulations of the complete siloxane capture processes were carried out to treat a realistic biogas stream, including the analysis of both absorption and regeneration columns. Process simulation results revealed that thermodynamics is the key property for the selection of ILs for siloxanes capture. Moreover, most of the selected ILs can satisfy silicon outlet concentration legislation (<5 mg_{Si}/Nm^3) in almost all the studied operating conditions. Last, solvent regeneration using air stripping column demonstrated the reversibility of the process in mild conditions of temperature (100 ºC) and vacuum

pressure (0.1 bar). In sum, ILs are proposed as promising siloxanes absorbents of siloxanes-containing streams, mainly focused on biogas upgrading.

Introduction

Biogas technology has emerged as an alternative to conventional energy resources due to the intensification of global warming [1]. Biogases are considered green, environmental, and valuable renewable fuel, including anaerobic digestion biogas (AD) and landfill gas (LFG), whose major constituent is methane (CH_4) [2]. Biogas also contains other undesirable chemicals such as CO_2, ammonia, H_2S, halogenated hydrocarbons, and siloxanes [3]. Siloxanes constitute the compounds that present most adverse effect on biogas utilization [1]. Siloxanes are volatile organic compounds that contains silicon-oxygen atoms joint (Si-O bonds) with organic groups such as methyl, or ethyl, among others [4]. They constitute a contaminant and an obstacle in biogas applications since they can severely damage equipment's, especially turbines, heat exchangers or gas engines [5] due the formation of silica (SiO_2) and microcrystalline quartz during combustion process that can be deposited at valves, spark plugs and cylinder heads [6]. For these reasons, it is necessary to remove traces of this contaminant from biogas before its application [7]. In fact, the maximum siloxane concentration in biogas (specified by engine manufacturers) is in the range 0.03-28 mg/m^3 [8]. Thus, different separation methods have been applied for siloxanes removal, among which stand out adsorption and absorption processes. Adsorption technology using activated carbons [9], silica gel [5] or zeolites presents some advantages on its use such as easy operation, strong adsorption ability (high adsorbent capacity), wide raw materials and low costs [10]. The removal efficiencies of this technology can reach up to 90-99% values [1]. However, some disadvantages found are the high regeneration temperature required, loss of adsorption capacity after regeneration process and a limited thermal regeneration efficiency due to the formation of polymerization products, that in most cases make regeneration unfeasible or require several units (one for use and one for regeneration). Additionally adsorbents are very sensitivity to moisture conditions [11]. Absorption processes usually employ methanol or Selexol® as physical solvents. Also siloxanes are effective removed by chemical absorption, since they can be destroyed with strong acids and bases and their removal efficiency increase with the type of contacting phase [12]. Their efficiencies are higher than 97% when using an organic solvent and lower than 95%

with an inorganic one [1]. The main drawbacks reported are the high investment and operation costs, environmental safety and corrosion, high energy required for removal process and absorbent regeneration. Moreover, siloxanes are difficult to be completely removed by physical absorption [8]. Other technologies that are being investigated for siloxanes removal are cryogenic condensation or membranes separation [1]. Cryogenic condensation efficiencies are governed by the operating temperature, reaching 99.3% for temperatures of -70 ºC and decreasing to 15-50% at higher ones (-25 ºC) [6]. It is a non-toxic technology with an easy operating way, but it implies high investment and operation costs, high energy required (to reach low temperatures) and it is economically feasible only when using high flow rate and high siloxanes loadings [13]. Membranes separations are simple and easy-operating technologies but they imply high investment costs, presenting risk of fouling, blocking and pollution [6]. In general, they present efficiencies higher than 80% [1].

It is well known that biogas contains CH_4 (60%) and carbon dioxide (40%) as well as other impurities described before. Therefore, it is important to remove not only siloxanes but also CO_2 present on biogas streams to increase the quality for its use [14]. Biogas upgrading concept was created focused on CO_2 elimination. It aims to increase the calorific value of the biogas to convert it to a higher fuel standard [15]. Regarding CO_2 removal methods, some disadvantages are found on the different technologies. Thus, physical absorption requires a huge amount of solvent to completely remove CO_2 [16]. Chemical absorption is a high energy-demanding technology to regenerate the amine-based solvent [17]. Adsorption process usually requires a complex technology since it uses pressure swing adsorption process [18]. Membranes technology presents low CO_2 selectivity and CH_4 purity reached are not enough for the separation [19]. Cryogenic separation needs high investment and operating cost for cooling the mixtures [20]. In the last decade, the kind of solvents called ionic liquids (ILs) have been widely studied as CO_2 absorbents due to their unique properties such as low vapor pressure, high thermal stability, high absorption capacity, among others [21]. It has been demonstrated competitive absorption capacities when compared with traditional solvents such as amine solutions [22, 23]. Recently, ILs have been applied on biogas upgrading due to the high CO_2/CH_4 selectivity values found [16, 24, 25]. To the best of our knowledge, no works involving siloxanes capture using ILs are reported up to date. In this context, our group has successfully used a multiscale research strategy -integrating both molecular and

process simulation- to design new gas separation processes based on ILs, including CO_2 [23, 26-28], NH_3 [29], H_2S [30], acetylene [31], toluene [31], among other solutes. As first step, a selection of the ILs able to absorb efficiently the solute can be done –among a huge database of cations and anions- by molecular simulation using COSMO-RS method [32]. Then, process simulations are applied to study the technical and economic viability of the gas capture operation based on the selected ILs at industrial scale, using the COSMO-based/Aspen Plus methodology [33]. For this purpose, ILUAM database was created allowing to use a collection of 100 ILs that did not exist on Aspen Properties databases [34].

The aim of this work is to evaluate the application of ILs as siloxanes absorbents based on molecular and process simulations. First, molecular simulation is employed to select ILs that can potentially capture the siloxanes among a wide sample of cations (35) and anions (35). COSMO-RS methodology is also used to analyze the solute-solvent intermolecular interactions, to understand the siloxane solubility in ILs. Then, Aspen Plus process simulator is applied to evaluate the behavior of selected ILs on siloxane absorption in commercial packing columns at process scale. Last, solvent regeneration process is studied to demonstrate the viability of IL reuse and to estimate related energy duty. A final concept test is performed by treating realistic multicomponent biogas flow with absorption technology based on ILs, to simultaneously capture siloxanes and CO_2, filling the quality standards of biomethane.

Computational details

COSMO-RS molecular simulation

ILs geometries were optimized using the independent counter ions (C+A) model at BP86/TZVP computational level using solvent effect by COSMO continuum solvation method as implicit in Turbomole. Siloxanes structures involved in this work (Table 1 collects the studied siloxane compounds, their physical properties, and the used nomenclature) were optimized at the same calculation level in gas phase. Once the geometries were optimized until their minimum energy level, a single point was performed in order to obtain the polarized charge distribution (σ-surface and σ-profile) stored in *.cosmo files. All the calculations required to obtain each *.cosmo file were carried out using Turbomole 4.5.2 and its graphical interface TurbomoleX v19. Then, COSMO-RS calculations were done using COSMOthermX software (version 19.0.4) and its parametrization BP_TZVP_19. Thus, σ-profile of pure compounds were obtained.

Regarding solute-IL interactions, Henry's law constants of siloxanes in ILs, excess Gibbs energy, entropy, and detailed contributions to excess enthalpies in equimolar siloxane-ILs mixtures were calculated. A detailed description of COSMO-RS calculations involving ILs can be found in our previous works [28-31, 35].

Aspen Plus process simulation

COSMO-based/Aspen Plus methodology was used to model siloxanes absorption and desorption operations based on ILs in both Equilibrium and Rate-Based modes of RADFRAC column. ILUAM (CA-RB) database was employed to incorporate selected ILs in Aspen Plus v11 process simulator since they are not available in extensive Aspen Properties databases). The compounds of gas inlet flow (siloxanes and CH_4) were used as default on Aspen Properties databases. In the case of siloxanes, it was completed the property package information by adding σ-profiles (SGPRF1-5) and COSMO volume (CSACVL) calculated with COSMO-RS method. First study comprises the evaluation of each siloxane separately with a gas flow containing 40 mg_{Si}/Nm^3 [1] of siloxane and balanced with CH_4 with a volume flow of 300 Nm^3/h (as average of biogas European plants [36]). The IL flow was maintained at 50 kg/h and it was evaluated the siloxanes concentration in the clean gas. The siloxanes limit in clean gas flows is 5 mg_{Si}/Nm^3, so it will be our reference to evaluate the behavior of selected ILs [37]. The total pressure was changed from 1 to 10 bar whereas temperature was maintained at 298.15 K. Regarding, siloxanes absorption column, it was modeled using RADFRAC in both Equilibrium and Rate-Based modes with 5 stages. The column height was 2 m of FLEXIPAC 700Y packing and the diameter was calculated to ensure a % approach to maximum capacity of 70%. Second study involves the complete process of siloxane capture from a realistic biogas stream (containing all the siloxanes in the composition found in Table 2), including the absorption column and regeneration stage by stripping (Scheme 1). Table 2 summarizes the design details of the simulated process.

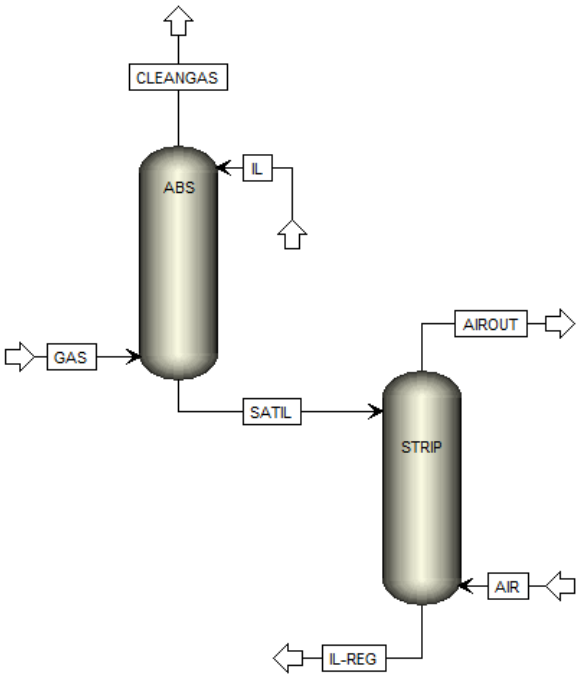

Scheme 1. Process diagram including capture process of siloxanes and IL regeneration steps

Table 1. Physical properties of siloxanes involved in this work

Siloxane	Formula	MW (g/mol)	P_{vap} (Pa) @ 298 K*	Melting Point (K)**	Boiling Point (K) **
Octamethyltrisiloxane (L3)	$C_8H_{24}O_2Si_3$	236.5	1076.0	186.8	425.7
Decamethyltetrasiloxane (L4)	$C_{10}H_{30}O_3Si_4$	310.8	483.0	197.1	467.6
Dodecamethylpentasiloxane (L5)	$C_{12}H_{36}O_4Si_5$	384.8	124.5	189.2	503.1
Hexamethylcyclotrisiloxane (D3)	$C_6H_{18}O_3Si_3$	222.5	47.0	336.8	407.3
Octamethylcyclotetrasiloxane (D4)	$C_8H_{24}O_4Si_4$	296.6	20.4	290.2	448.5
Decamethylcyclopentasiloxane (D5)	$C_{10}H_{30}O_5Si_5$	370.8	6.0	233.9	483.9

* Experimental data from [38]
**Experimental data collected from NIST available in Aspen Plus v11

Table 2. Operating conditions and column properties.

Column design	Absorption	Stripping
Height (m)	2	2
Packing type	FLEXIPAC 700Y	FLEXIPAC 700Y
Number of stages	5	5

Operating conditions	**Absorption**	**Stripping**
Gas volume flow (Nm^3/h)	300	8-40
Solvent mass flow (kg/h)	50	--
Temperature (K)	298.15	333.15-373.15
Pressure (bar)	1-10	0.1
Component	***Composition****	**--**
CH_4	40 %	--
CO_2	60 %	--

Composition (µg/Nm³)					
L3	L4	L5	D3	D4	D5
280	310	800	120	1900	124000

*Composition from [39]

Results

COSMO-RS molecular simulation

The prediction of thermodynamic properties of siloxane-ILs mixtures is possible thanks to COSMO-RS methodology [32]. It allows the quantification of interaction energy between surfaces with the polarized charge distribution (σ). σ-profile is the representation of polarized charge distribution in a histogram [40]. The chemical nature of the compounds can be rapidly analyzed by σ-profile representation. Thus, Figure 1 shows the σ-profile of the siloxanes involved in this work, comprising linear and cyclic ones. The three different regions in which it is divided are depicted on Figure 1. As general trend, σ-profile of all the compounds is dominated by a series of peaks in the non-polar region. Moreover, they also present some peaks in the H-bond acceptor region, which means a slight basic character due to the oxygen atoms in their structures. Minor differences are found between cyclic and linear-based siloxanes. It can be observed that in the case of linear compounds, they present a peak in the more positive region of the histogram; this is slightly stronger hydrogen bond acceptor capacity. Therefore, it can be anticipated that siloxanes will present favorable mixtures with non-polar compounds with acid character. Due to the observed negligible differences found between linear and cyclic compounds the following analysis will be centered on D3 compound.

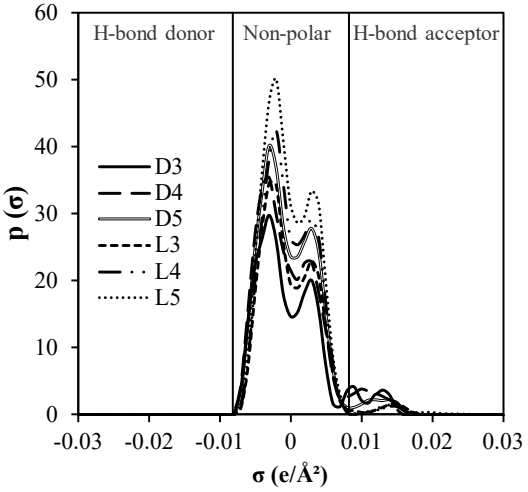

Figure 1. σ-profile of siloxanes studied on this work

Next stage of the study is focused on the selection of ILs with favorable properties for siloxanes absorption. Thus, a Henry's law constants screening among our huge database of ILs (>5000) has been carried out for the final selection. Figure 2 illustrates the obtained results in an IL sample of 30x30 combinations cation-anion for D3 siloxane. The complete names of cations and anions can be found in Table S1 of Supplementary Material. First, it is important to remark that lower Henry's law constants (dark green region) imply higher siloxanes solubility. As can be seen, K_H values are lower than 1 bar in the most part of the evaluated ILs. This means a high solubility of D3 in ILs, even higher than those reported for CO_2, H_2S, etc. [27, 28, 30]. Attending to the obtained results, it is clearly seen that both the cation and the anion has influence on D3 solubility. Therefore, it is important to select those that present favorable interactions. It seems that voluminous non-polar cations -such as quaternary phosphonium, ammonium or sulfonium-, in combination with bulky fluorinated anions with delocalized charge -such as $[FEP]^-$ and $[NTf_2]^-$- promotes the siloxane solubility in IL. Therefore, we selected a collection of favorable 6 cations and 6 anions to further analysis. Starting with the cations, we considered $[P_{666,14}]^+$ cation because of its favorable K_H. We also select $[N_{2HHH}]^+$, $[bmim]^+$, $[emim]^+$, $[bmpyr]^+$ and $[choline]^+$ cations in order to study the head group family effect on D3-ILs interactions. Regarding the anions, $[FEP]^-$ and $[NTf_2]^-$ were selected because they generally promote low K_H. In addition, ILs based on $[TCM]^-$ anion were also included due to their relatively low viscosity. Finally, it was incorporated a family of anions typically employed to chemically absorb CO_2 (present on biogas gas flows) such as $[2CNPyr]^-$, $[Ac]^-$ and $[Gly]^-$ [41-43].

Figure 3 represents the excess enthalpy of D3-IL equimolar binary mixture as a function of K_H of D3 in more than 1000 ILs, including those solvents previously selected. As can be seen, the curve presents an asymptotic behavior when values tend to K_H values of 0, increasing the siloxane solubility in IL (lower K_H) when the mixture becomes more exothermic (stronger attractive solute-solvent interactions). On the contrary, increasing endothermicity until a value close to 1 kcal/mol implies K_H leading to 10 bar; then, the entropy contribution becomes dominant drastically increasing the K_H values until >100 bar. It can be concluded that high solubilities are related to exothermic siloxane-IL mixtures; however, entropy may play a significant role for less favorable IL absorbents. Regarding the selected ILs, they cover the whole range of mixing behavior, from exothermic to endothermic mixtures. Next stage is focused on a detailed COSMO-RS analysis on the influence of the cation and the anion on the excess properties of siloxane-IL mixtures determining the absorption phenomena.

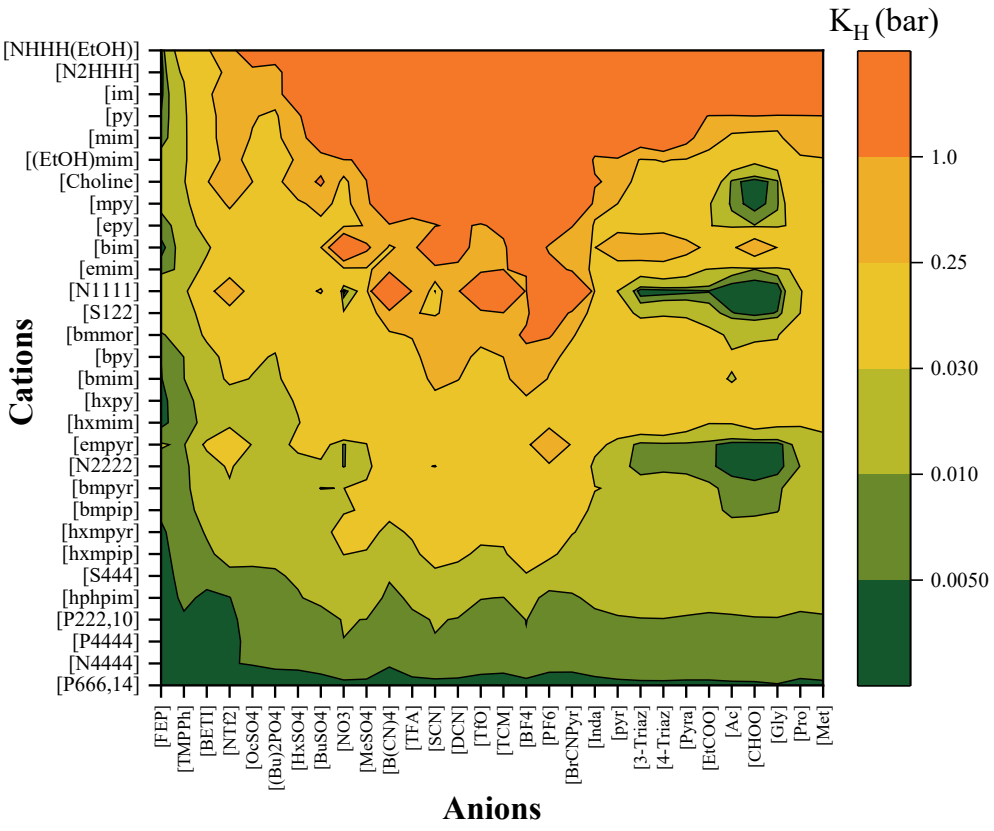

Figure 2. Henry's law constants (K_H) screening of D3 in 900 ILs at 298.15 K

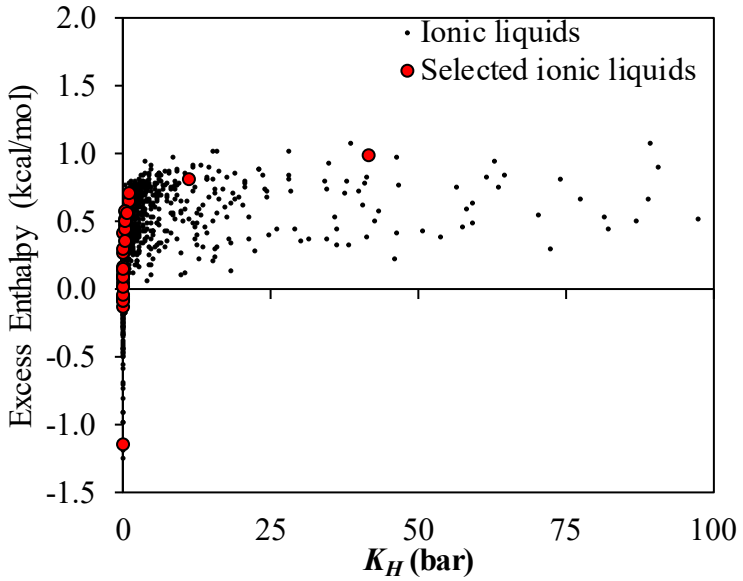

Figure 3. Excess molar enthalpies (H^E) of equimolar D3-ILs mixtures versus Henry's law constants (K_H) by COSMO-RS at 298.15 K.

Figure 4A shows the excess molar enthalpies, entropies and Gibbs free energies of D3-IL for series of selected anions with the fixed cation $[P_{666,14}]^+$. As can be seen, the enthalpy is clearly governing the interaction between D3 and these ILs. From those selected, $[FEP]^-$ anion is the only one that exhibits a negative value of excess Gibbs free energy, whereas the rest of the anions present positive ones, being ordered as a function of excess enthalpy values. It is important to remark that entropy contribution is unfavorable only in the case of $[P_{666,14}][FEP]$, whereas the rest of the ILs present a favorable entropy contribution to the mixture. Once it is concluded that enthalpy is governing the absorption process in this IL sample with common cation, Figure 4B reveals the intermolecular interaction contributions to excess molar enthalpy in D3-ILs. As can be seen, polar/electrostatic forces (Misfit) are the main contribution to the enthalpy, computing the 60% of the total. Those ILs that present hydrogen bond acceptor groups ($[Gly]^-$, $[Ac]^-$ or $[2CNPyr]^-$) have unfavorable influence on D3-ILs mixture, probably due to repulsive D3-anion interactions. Despite having endothermic mixtures, it can be seen (Figure 4B) that K_H values are between 0.001-0.005 bar, which means that D3 solubility is very high in all $[P_{666,14}]$-based ILs, not being strongly influenced by the selected anion.

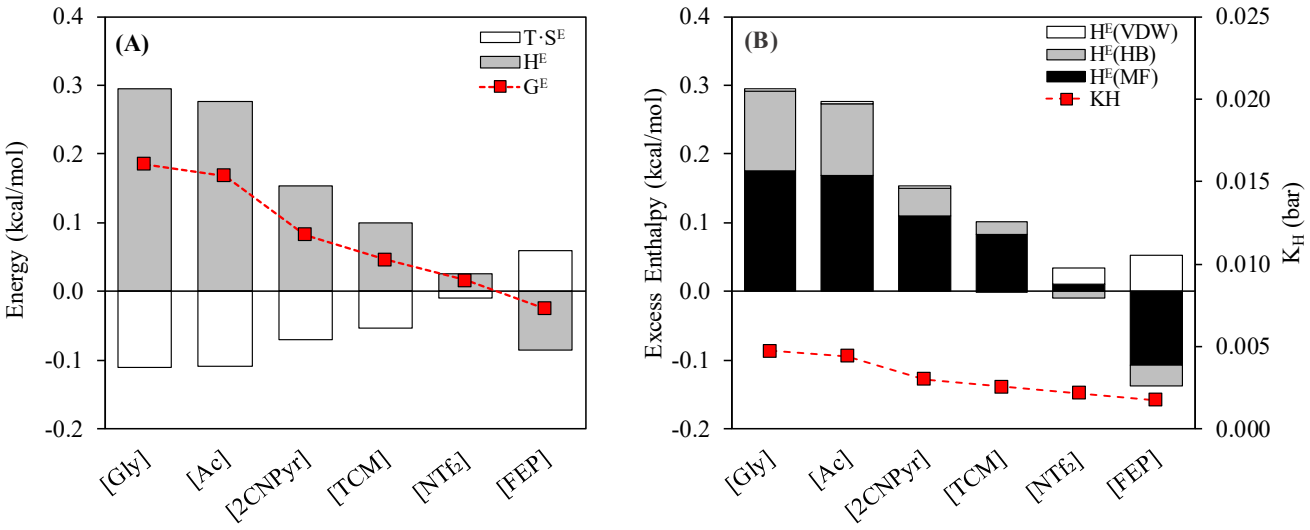

Figure 4. Excess molar enthalpies, entropies and Gibbs energies **(A)** and H^E contributions (Van der Waals, Hydrogen Bond and Misfit) *vs* K_H values **(B)** of $[P_{666,14}]^+$ cation with different selected anions and D3 siloxane at 298.15 K computed by COSMO-RS.

Figure 5A shows excess enthalpy and entropy contributions to excess Gibbs energy for D3-ILs systems with the common anion $[FEP]^-$. In the case of the cation influence, we observed significant both enthalpic and entropic contributions to excess Gibbs energy, so no one is clearly governing the process. The cases of the $[P_{666,14}][FEP]$ and $[N_{2HHH}][FEP]$ presents negative excess Gibbs free energy of mixture with D3, in contrast to the rest of the cations considered. It is interesting to note that D3-$[P_{666,14}][FEP]$ system presents an almost ideal mixing behavior (H^E and $-TS^E$ close to 0) whereas D3-$[N_{2HHH}][FEP]$ presents significant favorable enthalpic and unfavorable entropic changes with mixing phenomena, which cancel each other, leading to G^E values close to zero. Figure 5B revealed the contributions to excess molar enthalpy for each IL system. In this case, we observe significant attractive interactions between D3 and the hydrogen bond donor group of some cations ($[Choline]^-$, $[N_{2HHH}]^+$). Regarding K_H values for D3-IL series with common $[FEP]^-$ anion (Figure 5B), they cover a wide range from 0.001 to 0.025 bar, so it seems that cation selection has a great influence on siloxane-IL mixing behavior and, consequently, on D3 solubility in IL.

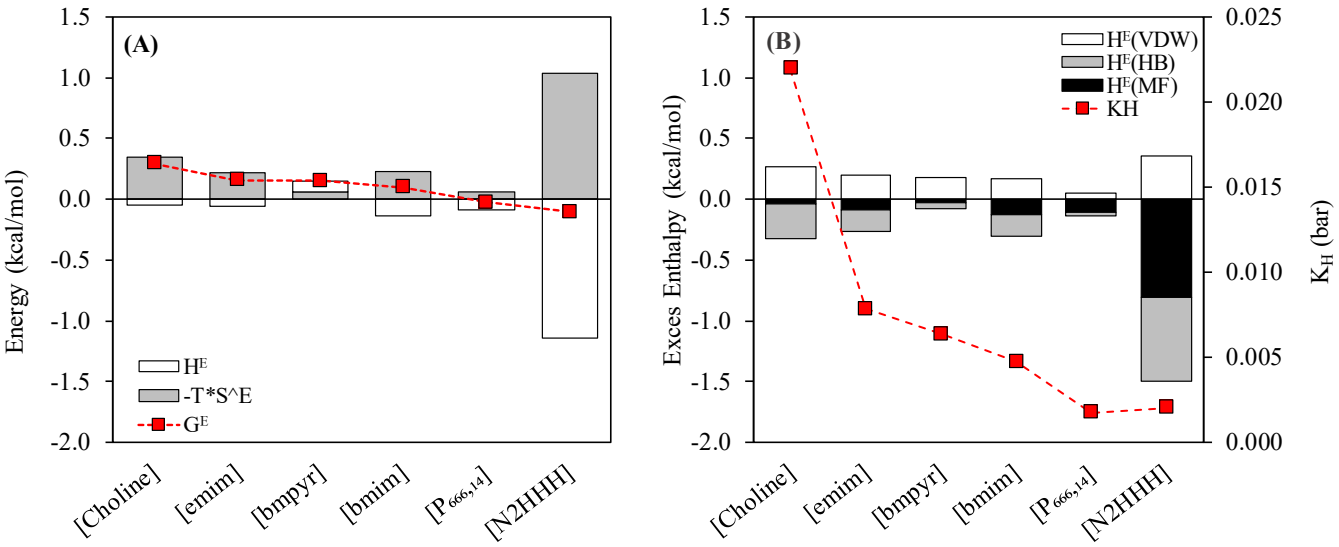

Figure 5. Excess molar enthalpies, entropies, and Gibbs energies **(A)** and H^E contributions (Van der Waals, Hydrogen Bond and Misfit) *vs* K_H values **(B)** of $[FEP]^-$ anion with different selected cations and D3 siloxane at 298.15 K computed by COSMO-RS.

From previous analysis, a collection of 9 ILs were selected as promising siloxanes absorbents. Table 3 collects their properties such as molecular weight, D3 Henry's law constant and viscosity. As can be seen, they were selected attending to low K_H values of D3 (as reference) in IL, which means high siloxane solubility. Moreover, we decided to include two ILs based on $[Ac]^-$ with higher K_H since they are commonly used in CO_2 capture as chemical absorbents [42]. Thus, it can be evaluated an IL system able to simultaneously remove both CO_2 and siloxanes from biogas streams. The rest of the ILs were selected based on their low viscosity values to analyze the possible mass transfer kinetic restrictions of the operation. A huge range of molecular weights was also selected to investigate its influence on the absorption process. Last, it is important to remark that all the selected ILs are included in ILUAM database [34], being used the CA-RB databank on following Aspen Plus calculations.

Table 3. Selected ILs properties

Ionic Liquids	***MW* (g/mol)**	**D3 K_H (bar)[a]**	**μ (cP)[b] @ 298.15 K**
$[P_{666,14}][FEP]$	928.9	0.0018	353.1
$[P_{666,14}][NTf_2]$	764.0	0.0022	342.9
[emim][FEP]	556.2	0.0078	59.7
[emim][Ac]	170.2	0.0138	138.5
[bmim][Ac]	198.3	0.0289	447.2
$[bmim][NTf_2]$	419.4	0.0340	51.4
$[emim][NTf_2]$	391.3	0.0941	34.1
[bmim][TCM]	229.3	0.1822	28.5
[emim][TCM]	201.2	0.9312	14.6

[a] K_H estimated by COSMO-RS
[b] Experimental viscosity from ILUAM [14]

To complete current COSMO-RS analysis, Figure 6 and 7 show the excess enthalpy and entropy contributions to excess Gibbs energy of the solute-solvent equimolar binary mixtures, including all the siloxanes of the study (Table 1) with [emim][FEP] due to its low K_H and [bmim][Ac] as reference of CO_2 chemical absorbent. As can be seen, enthalpic contribution seems to govern the absorption process in [emim][FEP] case (Figure 6A), whereas entropic changes do it in [bmim][Ac] (Figure 7A). The COSMO-RS analysis shows that cyclic siloxanes (D3, D4 and D5) present higher solubility in the ILs (lower K_H values) than linear siloxanes (L3, L4 and L5). The length of molecule seems to present a minor effect on cyclic siloxanes solubility in ILs, whereas it plays a relevant role in linear siloxanes, significantly increasing the gas solubility for linear siloxane of higher molecular size. Regarding contributions to excess enthalpy, in the case of [emim][FEP] hydrogen bond contribution has a positive effect on siloxanes solubility whereas in the case of [bmim][Ac] it presents a negative effect. In any case, it can be concluded that all the siloxanes present very high gas solubility in ILs independently of their nature and the selected ILs. Next stage will be centered on the evaluation of selected ILs on realistic siloxane absorption in commercial packed columns.

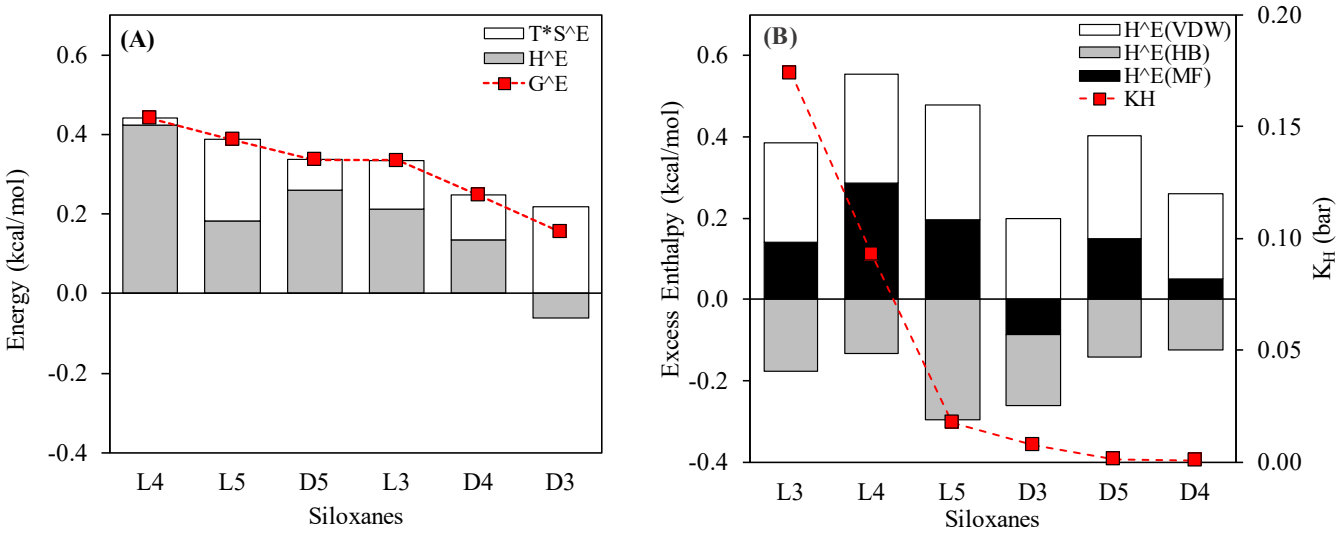

Figure 6. Excess molar enthalpies, entropies, and Gibbs energies **(A)** and H^E contributions (Van der Waals, Hydrogen Bond and Misfit) *vs* K_H values **(B)** of [emim][FEP] with different siloxanes at 298.15 K computed by COSMO-RS.

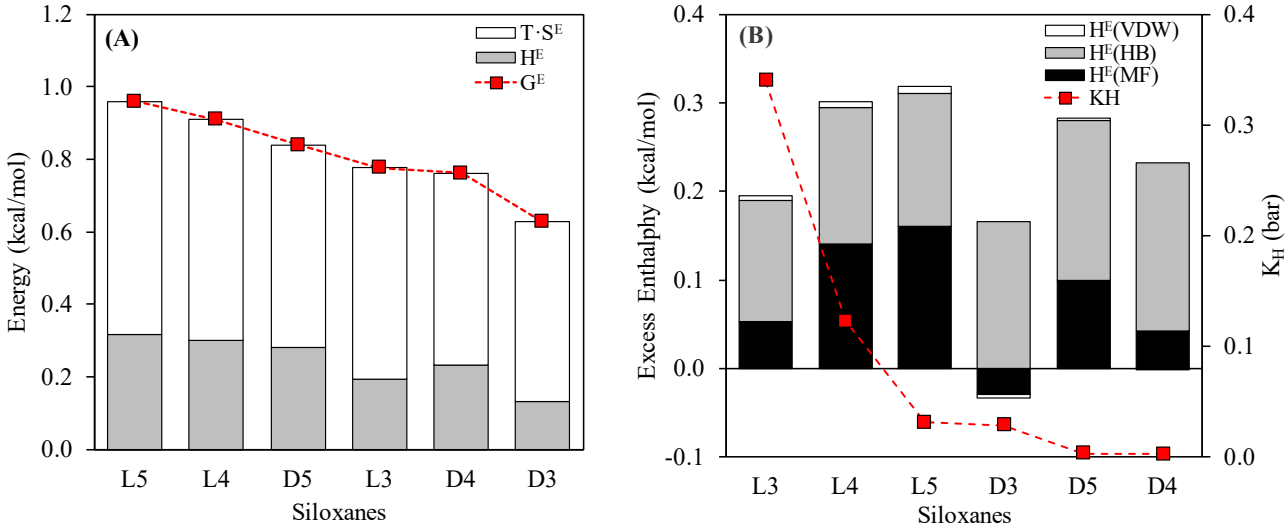

Figure 7. Excess molar enthalpies, entropies, and Gibbs energies **(A)** and H^E contributions (Van der Waals, Hydrogen Bond and Misfit) **(B)** of [bmim][MeCOO] with different siloxanes at 298.15 K computed by COSMO-RS.

Aspen Plus process simulation

The first step was to evaluate the process performance of selected ILs in siloxane capture by using a commercial packed column. Series of synthetic streams of 300 Nm^3/h composed by methane and 40 mg_{Si}/Nm^3 of each studied siloxane are put in contact with 50 kg/h of IL in an absorption column at Table 2 conditions. Figure 8 depicts the obtained outlet concentration of the different siloxanes at 1 bar of total pressure and 298 K.

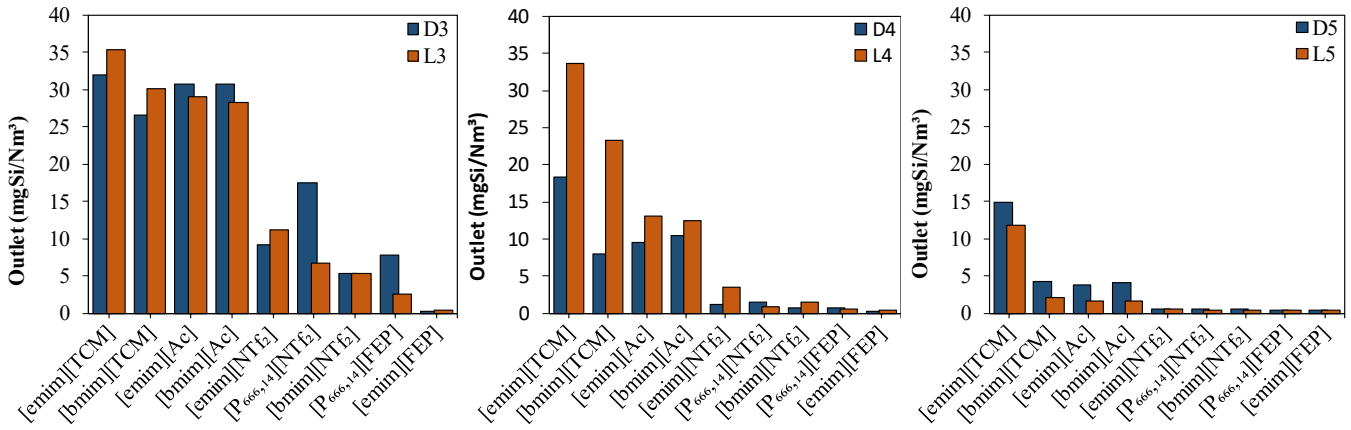

Figure 8. Siloxane outlet concentrations after absorption column at 1 bar and 298 K for synthetic mixtures of CH_4/Siloxane with 40 mg/Nm^3 of correspondent compound.

Starting with D3 and L3 cases, it is concluded that ILs present a wide different absorbent behavior, from almost no siloxane recovery in the case of [emim][TCM] to nearly complete recovery in [emim][FEP]. The anion is clearly dominating the absorption efficiency of the ILs, being the order $[FEP]^-$ > $[NTf_2]^-$ > $[Ac]^-$ > $[TCM]^-$. If we establish a minimum outlet concentration of 5 $mgSi/Nm^3$ as a limit commonly specified for grid injection [37], $[FEP]^-$ and $[NTf_2]^-$ anions are able to reach this specification for D3 and L3 at ambient pressure. Regarding the effect of the siloxane employed, as expected the recovery remarkably increases with the siloxane size (D5>D4>D3). The differences between linear and cyclic siloxanes are minor and vary from case to case, being related to the mass solubility of the siloxane in the correspondent IL (**Table 4)**. It should be emphasized that, at the given operating conditions, the benchmark value (5 mg_{Si}/Nm^3) of outlet concentration is reached (even overcome) for all siloxanes using some of selected ILs: [bmim][NTf_2], [$P_{666,14}$][FEP] and [emim][FEP].

Table 4. Equilibrium solubility of the different siloxanes in the ILs at 298 K and 10^{-5} bar of partial pressure (1 bar of total pressure).

IL	Solubility (g/kg_{IL})					
	D3	**L3**	**D4**	**L4**	**D5**	**L5**
[emim][TCM]	0.16	0.10	0.62	0.17	0.97	1.25
[bmim][TCM]	0.27	0.21	1.26	0.48	2.52	4.46
[emim][Ac]	0.19	0.24	1.27	1.03	3.18	6.63
[bmim][Ac]	0.20	0.28	1.40	1.28	3.84	8.81
[emim][NTf_2]	0.84	0.78	4.80	2.33	18.68	68.23
[$P_{666,14}$][NTf_2]	0.54	1.31	4.70	9.21	27.88	167.46
[bmim][NTf_2]	1.20	1.30	7.48	4.38	30.89	173.10
[$P_{666,14}$][FEP]	1.05	2.43	9.22	16.23	55.63	266.79
[emim][FEP]	18.70	15.01	98.02	53.58	320.42	1064.67

After analyzing the operation at 1 bar, the effect of pressure on the siloxane absorption in IL is evaluated. Figure 9 presents the outlet concentration of the absorption column at the different total pressures (1, 5 and 10 bar) for three of the ILs studied (rest of the ILs can be found in Figure S1 of Supplementary Material).

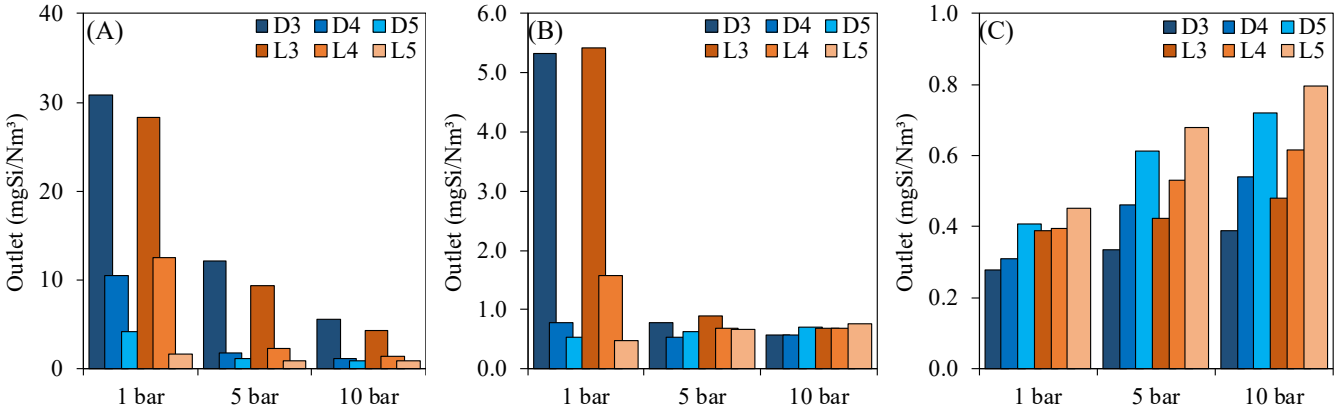

Figure 9. Outlet siloxane concentration at different pressures for [bmim][Ac] (A), [bmim][NTf_2] (B) and [emim][FEP] (C).

In the case of [bmim][Ac] (Figure 9A), an increase of the operating pressure greatly increases the siloxane capture. Thus, the outlet concentration of all studied siloxanes reaches values below 5 mg_{Si}/Nm^3 at 10 bar. In the case of [bmim][NTf_2] (where remarkably lower outlet concentration than [bmim][Ac] is observed), the absorption efficiency increases from 1 to 5 bar, remaining almost unchanged from 5 to 10 bar. This is explained because the solubility at higher pressures for all siloxanes (Table S2 of Supplementary Material) is far above the total amount of siloxane available in the inlet gas stream, so increasing the pressure is very inefficient. In the case of [emim][FEP]

(which allows very low siloxane outlet concentration), an opposite pressure effect is observed: the siloxane uptake decreases at higher pressure, rising its outlet concentration. This effect can be explained because, although the selectivity of siloxane over methane is very high (> 10^5 in most cases, Table S3 in Supplementary Material), increasing the pressure up to 5 bar almost does not change the amount of siloxane absorbed, whereas still increases the absorption of methane, lowering the CO_2/CH_4 selectivity, and implying slightly higher concentration of siloxane in the clean gas.

Finally, the complete process of siloxane capture (Scheme 1) was simulated by COSMO-based/Aspen approach using real biogas stream, containing all six siloxanes, carbon dioxide and methane [38], in the composition detailed in Table 2. This biogas is typical from wastewater treatment plants, with an average siloxane composition near 40 mg/m^3 ,where D4 and D5 is usually above 90% of total siloxanes [1]. Figure 10 presents the outlet concentration of total siloxane in the absorption column at 1 bar of total pressure and 298 K for different absorbent mass flows using selected IL.

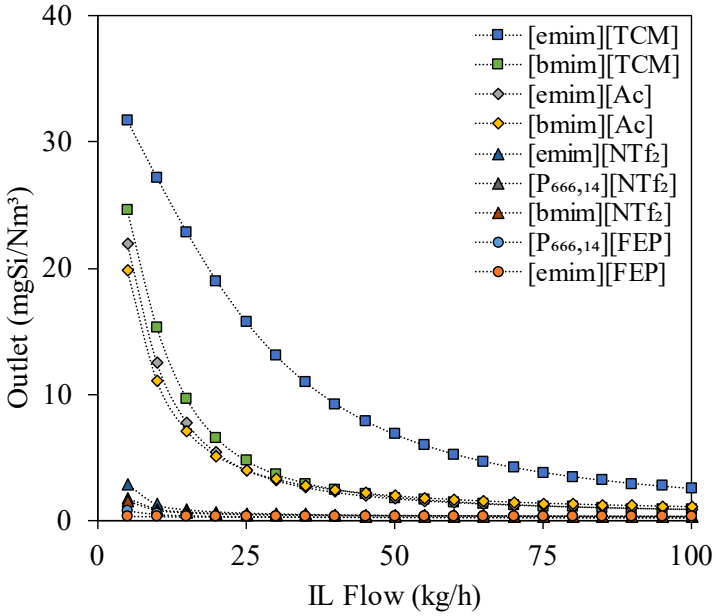

Figure 10. Effect of the ILs mass flow on the siloxane outlet concentration of absorption columns at 298 K and 1 bar.

The ILs can be classified attending to the absorbent behavior observed for pure D5 (Figure 8). First, $[Ac]^-$ and $[TCM]^-$ anion based ILs present comparatively low siloxane capture, finding that an increment in the IL mass flow clearly improves the siloxanes separation. In contrast, for ILs based on $[FEP]^-$ and $[NTf_2]^-$ anions, the siloxane solubility is very high. For this reason, the amount of IL required to completely remove the

siloxanes from gas streams is very low; then, an increase in the liquid flow does not have any practical effect on the separation efficiency, achieving a removal of 99% in the case of [emim][FEP] for a flow such low like 5 kg/h of IL.

However, such affinity toward siloxanes make the regeneration of the IL more difficult. In current separation proposal (Scheme 1), the solvent regeneration was attempted by using a small air stripping column (Table 2). Two ILs with clear different behavior were evaluated, [emim][FEP] and [bmim][Ac], being the first IL the best siloxane absorbent and the later an IL proposed for biogas upgrading , due to its favorable CO_2 chemical absorption [44]. For this study, the saturated IL was put in contact with an air stream at a total pressure of 0.1 bar at different operating temperatures (60, 70 and 80 ºC).

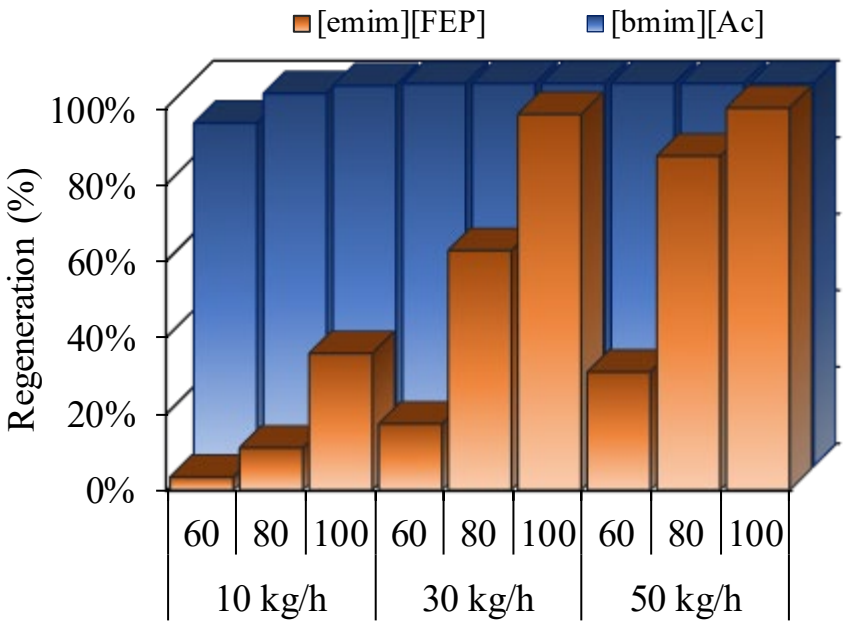

Figure 11. IL regeneration at total pressure of 0.1 bar and different temperatures (60, 80 and 100ºC) and stripping air flow (10, 20 and 30 kg/h) for [emim][FEP] (front) and [bmim][Ac] (back).

Figure 11 depicts the percentage of siloxane removed from the exhausted IL stream in the regeneration column, as a function of the temperature and the stripping air flow. In the case of the best absorbent, [emim][FEP], as expected, an increase in the operating temperature clearly improves the regeneration, due the lower solubility of siloxanes at higher temperatures. The same occurs when increasing the stripping flow employed, that

reduces the partial pressure of siloxane in the gas phase, promoting a more efficient IL regeneration. In the case of [emim][FEP], the regeneration needs at least 100ºC and high air flows (50 kg/h) to reach a reasonable siloxane recovery value (> 90%). In the case of [bmim][Ac], the IL is almost completely regenerated at all the studied conditions, due to its relatively lower siloxanes affinity.

It should be noted that the very high uptake of siloxanes in [emim][FEP] (200 g/kg at 0.5 g/m^3 D4 and 298 K and 1 bar) is comparable or even higher than some of conventional adsorbents, such activated carbons (50-300 g/kg at similar conditions [38]) or zeolites (100-200 g/kg at similar conditions [38]). An improvement in the application of this IL in siloxane capture may be its immobilization in a porous solid to generate supported or encapsulated ILs [43, 45]. It would allow using ILs in gas-solid separation technology, with materials presenting similar uptake capacity than conventional adsorbents but remarkably easier regeneration (the regeneration temperatures commonly used for adsorbent is up to 250 ºC [3]. In the case of [bmim][Ac], we noticed that, despite having lower performance than other selected ILs, all the solvent requirements and regeneration conditions needed for siloxane capture process are lower than those needed for CO_2 capture in a biogas application [44], so a great advantage is found being able to simultaneously remove both CO_2 and siloxanes in biogas upgrading applications.

Conclusions

COSMO-based/Aspen Plus methodology was successfully applied to reveal the promising application of ILs to siloxanes capture, centered on biogas upgrading technology. Molecular simulation results using COSMO-RS method suggested the high affinity of ILs for linear and cyclic siloxane gas compounds, obtaining Henry's law constants in the range 0.001-1 bar. Intermolecular interaction analysis of siloxane-IL mixtures let us conclude that the absorption phenomenon is governed by excess enthalpy in most favorable ILs. The results showed that ILs with fluorinated anions present the best behavior from the thermodynamic point of view. COSMO-RS analysis was extensive to all the involved siloxanes resulting in almost the same conclusions. ILs tested on process simulation stage were selected based on not only thermodynamics (low K_H), but also low *MW* and low viscosity. Process simulation results in rigorous absorption packed column revealed that ILs performance is ordered as a function of the anion, being $[FEP]^-$

and $[NTf_2]^-$ those that exhibit the highest siloxane separation efficiency, due to their high siloxane gas solubility. The observed effects of operating pressure in the column were related with siloxane/CH_4 selectivity. Finally, simulations of the complete siloxane capture process using a real biogas stream (including all the siloxanes and CO_2) confirmed the previous extracted conclusions. ILs regeneration using stripping columns with air demonstrated the reversibility of the process in mild conditions of temperature (100 ºC) and pressure (0.1 bar).

Acknowledgments

The authors are very grateful to Ministerio de Economía y Competitividad (MINECO) of Spain (project CTQ2017-89441-R) and Comunidad de Madrid (P2018/EMT4348) for financial support. We also thank Centro de Computación Científica de la Universidad Autónoma de Madrid for computational facilities.

References

1. Shen, M., Y. Zhang, D. Hu, J. Fan, and G. Zeng, *A review on removal of siloxanes from biogas: with a special focus on volatile methylsiloxanes.* Environ Sci Pollut Res Int, 2018. **25**(31): p. 30847-30862.
2. Souza, Nelson, Ivan Werncke, Cleber Marques, Reinaldo Bariccatti, Reginaldo Ferreira Santos, Carlos Nogueira, and Doglas Bassegio, *Electric energy micro-production in a rural property using biogas as primary source.* Renewable and Sustainable Energy Reviews, 2013. **28**: p. 385-391.
3. Elwell, Anthony C., Nada H. Elsayed, John N. Kuhn, and Babu Joseph, *Design and analysis of siloxanes removal by adsorption from landfill gas for waste-to-energy processes.* Waste Management, 2018. **73**: p. 189-196.
4. Kapoor, R., P. Ghosh, M. Kumar, and V. K. Vijay, *Evaluation of biogas upgrading technologies and future perspectives: a review.* Environmental Science and Pollution Research, 2019. **26**(12): p. 11631-11661.
5. Meng, Zeyou, Yuheng Liu, Xiao Li, and Zichuan Ma, *Removal of siloxane (L2) from biogas using methyl-functionalised silica gel as adsorbent.* Chemical Engineering Journal, 2020. **389**: p. 124440.
6. Gao, Ruiling, Shikun Cheng, and Zifu Li, *Research progress of siloxane removal from biogas.* International Journal of Agricultural and Biological Engineering, 2017. **10**: p. 30-39.
7. Lee, Ilsu and Bruce E. Rittmann, *Using Focused Pulsed Technology to Remove Siloxane from Municipal Sewage Sludge.* Journal of Environmental Engineering, 2016. **142**(1): p. 04015056.
8. Pierce, Jeffrey, *Siloxanes in Landfill and Digester Gas Update*, in *27th Annual SWANA LFG Symposium*. 2004: California.

9. Tran, Vu Tung Lam, Patrick Gélin, Corinne Ferronato, Jean–Marc Chovelon, Ludovic Fine, and Georgeta Postole, *Adsorption of linear and cyclic siloxanes on activated carbons for biogas purification: Sorbents regenerability.* Chemical Engineering Journal, 2019. **378**: p. 122152.
10. Huppmann, Rene, Horst Werner Lohoff, and Horst Friedrich Schröder, *Cyclic siloxanes in the biological waste water treatment process – Determination, quantification and possibilities of elimination.* Fresenius' Journal of Analytical Chemistry, 1996. **354**(1): p. 66-71.
11. Soreanu, Gabriela, Béland M, Patricia Falletta, Edmonson K, Svoboda L, Al-Jamal M, and Seto P, *Approaches concerning siloxane removal from biogas - A review.* Canadian Biosystems Engineering / Le Genie des biosystems au Canada, 2011. **53**: p. 8.1-8.18.
12. Charry Prada, Iran D., Rodrigo Rivera-Tinoco, and Chakib Bouallou, *Biogas industry: Novel acid gas removal technology using a superacid solvent. Process design, unit specification and feasibility study compared with other existing technologies.* Chemical Engineering Research and Design, 2020. **154**: p. 212-231.
13. Hagmann, Manfred, E. Hesse, P. Hentschel, and T. Bauer, *Purification of biogas-removal of volatile silicones.* Proceedings of 8th International Waste Management and Landfill Symposium (Sardinia 2001), 2001. **2**: p. 641-644.
14. Adnan, Amir Izzuddin, Mei Yin Ong, Saifuddin Nomanbhay, Kit Wayne Chew, and Pau Loke Show, *Technologies for Biogas Upgrading to Biomethane: A Review.* Bioengineering (Basel, Switzerland), 2019. **6**(4).
15. Sun, Qie, Hailong Li, Jinying Yan, Longcheng Liu, Zhixin Yu, and Xinhai Yu, *Selection of appropriate biogas upgrading technology-a review of biogas cleaning, upgrading and utilisation.* Renewable and Sustainable Energy Reviews, 2015. **51**: p. 521-532.
16. Garcia-Gutierrez, P., J. Jacquemin, C. McCrellis, I. Dimitriou, S. F. R. Taylor, C. Hardacre, and R. W. K. Allen, *Techno-Economic Feasibility of Selective CO2 Capture Processes from Biogas Streams Using Ionic Liquids as Physical Absorbents.* Energy & Fuels, 2016. **30**(6): p. 5052-5064.
17. Leonzio, Grazia, *Upgrading of biogas to bio-methane with chemical absorption process: simulation and environmental impact.* Journal of Cleaner Production, 2016. **131**: p. 364-375.
18. Ho, Minh T., Guy W. Allinson, and Dianne E. Wiley, *Reducing the Cost of CO2 Capture from Flue Gases Using Pressure Swing Adsorption.* Industrial & Engineering Chemistry Research, 2008. **47**(14): p. 4883-4890.
19. Harasimowicz, M., P. Orluk, G. Zakrzewska-Trznadel, and A. G. Chmielewski, *Application of polyimide membranes for biogas purification and enrichment.* Journal of Hazardous Materials, 2007. **144**(3): p. 698-702.
20. Grande, Carlos and Richard Blom, *Cryogenic Adsorption of Methane and Carbon Dioxide on Zeolites 4A and 13X.* Energy & Fuels, 2014. **28**: p. 6688-6693.
21. Rogers, Robin D. and Kenneth R. Seddon, *Ionic Liquids--Solvents of the Future?* Science, 2003. **302**(5646): p. 792-793.
22. Aghaie, M., N. Rezaei, and S. Zendehboudi, *A systematic review on CO2 capture with ionic liquids: Current status and future prospects.* Renewable & Sustainable Energy Reviews, 2018. **96**: p. 502-525.
23. de Riva, J., V. Ferro, C. Moya, M. A. Stadtherr, J. F. Brennecke, and J. Palomar, *Aspen Plus supported analysis of the post-combustion CO2 capture by chemical absorption using the [P2228][CNPyr] and [P66614][CNPyr]AHA Ionic Liquids.* International Journal of Greenhouse Gas Control, 2018. **78**: p. 94-102.

24. Xie, Yujiao, Johanna Björkmalm, Chunyan Ma, Karin Willquist, Johan Yngvesson, Ola Wallberg, and Xiaoyan Ji, *Techno-economic evaluation of biogas upgrading using ionic liquids in comparison with industrially used technology in Scandinavian anaerobic digestion plants.* Applied Energy, 2018. **227**: p. 742-750.
25. Xie, Y. J., C. Y. Ma, X. H. Lu, and X. Y. Ji, *Evaluation of imidazolium-based ionic liquids for biogas upgrading.* Applied Energy, 2016. **175**: p. 69-81.
26. de Riva, Juan, José Suarez-Reyes, Daniel Moreno, Ismael Díaz, Víctor Ferro, and José Palomar, *Ionic liquids for post-combustion CO2 capture by physical absorption: Thermodynamic, kinetic and process analysis.* International Journal of Greenhouse Gas Control, 2017. **61**: p. 61-70.
27. Palomar, J., M. Larriba, J. Lemus, D. Moreno, R. Santiago, C. Moya, J. de Riva, and G. Pedrosa, *Demonstrating the key role of kinetics over thermodynamics in the selection of ionic liquids for CO2 physical absorption.* Separation and Purification Technology, 2019. **213**: p. 578-586.
28. Palomar, Jose, Maria Gonzalez-Miquel, Alicia Polo, and Francisco Rodriguez, *Understanding the Physical Absorption of CO2 in Ionic Liquids Using the COSMO-RS Method.* Industrial & Engineering Chemistry Research, 2011. **50**(6): p. 3452-3463.
29. Palomar, Jose, Maria Gonzalez-Miquel, Jorge Bedia, Francisco Rodriguez, and Juan J. Rodriguez, *Task-specific ionic liquids for efficient ammonia absorption.* Separation and Purification Technology, 2011. **82**: p. 43-52.
30. Santiago, Rubén, Jesús Lemus, Ana Xiao Outomuro, Jorge Bedia, and José Palomar, *Assessment of ionic liquids as H2S physical absorbents by thermodynamic and kinetic analysis based on process simulation.* Separation and Purification Technology, 2020. **233**: p. 116050.
31. Santiago, R., J. Bedia, D. Moreno, C. Moya, J. de Riva, M. Larriba, and J. Palomar, *Acetylene absorption by ionic liquids: A multiscale analysis based on molecular and process simulation.* Separation and Purification Technology, 2018. **204**: p. 38-48.
32. Klamt, Andreas, *Conductor-like screening model for real solvents: a new approach to the quantitative calculation of solvation phenomena.* The Journal of Physical Chemistry, 1995. **99**(7): p. 2224-2235.
33. Lin, Shiang-Tai and Stanley I Sandler, *A priori phase equilibrium prediction from a segment contribution solvation model.* Industrial & engineering chemistry research, 2002. **41**(5): p. 899-913.
34. Ferro, V. R., C. Moya, D. Moreno, R. Santiago, J. de Riva, G. Pedrosa, M. Larriba, I. Diaz, and J. Palomar, *Enterprise Ionic Liquids Database (ILUAM) for Use in Aspen ONE Programs Suite with COSMO-Based Property Methods.* Industrial & Engineering Chemistry Research, 2018. **57**(3): p. 980-989.
35. Bedia, Jorge, Elia Ruiz, Juan de Riva, Victor R. Ferro, Jose Palomar, and Juan Jose Rodriguez, *Optimized ionic liquids for toluene absorption.* AIChE Journal, 2013. **59**(5): p. 1648-1656.
36. Association, European Biogas, *EBA Annual Report.* Journal, 2019.
37. Mandereau, Arthur Wellinger and Christophe, *Selection and Evaluation of Ionic Liquids for Siloxanes Capture based on Molecular and Process Simulation.* Journal, 2015.
38. Wang, Gang, Zhongshen Zhang, and Zhengping Hao, *Recent advances in technologies for the removal of volatile methylsiloxanes: A case in biogas purification process.* Critical Reviews in Environmental Science and Technology, 2019. **49**(24): p. 2257-2313.

39. Raich-Montiu, J., C. Ribas-Font, N. de Arespacochaga, E. Roig-Torres, F. Broto-Puig, M. Crest, L. Bouchy, and J. L. Cortina, *Analytical methodology for sampling and analysing eight siloxanes and trimethylsilanol in biogas from different wastewater treatment plants in Europe.* Analytica Chimica Acta, 2014. **812**: p. 83-91.
40. Klamt, Andreas, Frank Eckert, and Wolfgang Arlt, *COSMO-RS: An Alternative to Simulation for Calculating Thermodynamic Properties of Liquid Mixtures.* Annual Review of Chemical and Biomolecular Engineering, 2010. **1**(1): p. 101-122.
41. Seo, Samuel, Mauricio Quiroz-Guzman, M. Aruni DeSilva, Tae Bum Lee, Yong Huang, Brett F. Goodrich, William F. Schneider, and Joan F. Brennecke, *Chemically Tunable Ionic Liquids with Aprotic Heterocyclic Anion (AHA) for CO2 Capture.* The Journal of Physical Chemistry B, 2014. **118**(21): p. 5740-5751.
42. Moya, Cristian, Noelia Alonso-Morales, Miguel A. Gilarranz, Juan J. Rodriguez, and Jose Palomar, *Encapsulated Ionic Liquids for CO2 Capture: Using 1-Butyl-methylimidazolium Acetate for Quick and Reversible CO2 Chemical Absorption.* ChemPhysChem, 2016. **17**(23): p. 3891-3899.
43. Santiago, Rubén, Jesús Lemus, Cristian Moya, Daniel Moreno, Noelia Alonso-Morales, and José Palomar, *Encapsulated Ionic Liquids to Enable the Practical Application of Amino Acid-Based Ionic Liquids in CO2 Capture.* ACS Sustainable Chemistry & Engineering, 2018. **6**(11): p. 14178-14187.
44. Hospital-Benito, D., J. Lemus, C. Moya, R. Santiago, and J. Palomar, *Process analysis overview of ionic liquids on CO2 chemical capture.* Chemical Engineering Journal, 2020. **390**: p. 124509.
45. Santiago, Ruben, Jesus Lemus, Daniel Hospital-Benito, Cristian Moya, Jorge Bedia, Noelia Alonso-Morales, Juan J. Rodriguez, and Jose Palomar, *CO2 Capture by Supported Ionic Liquid Phase: Highlighting the Role of the Particle Size.* Acs Sustainable Chemistry & Engineering, 2019. **7**(15): p. 13089-13097.